Environmental Pollution 279 (2021) 116882

Contents lists available at ScienceDirect

Environmental Pollution

journal homepage: www.elsevier.com/locate/envpol

Recent trends in premature mortality and health disparities attributable to ambient $PM_{2.5}$ exposure in China: 2005–2017☆

Ming Liu [a, f], Rebecca K. Saari [a, b, *], Gaoxiang Zhou [a, c], Jonathan Li [a, d], Ling Han [e], Xiangnan Liu [c]

[a] Department of Geography and Environmental Management, University of Waterloo, Waterloo, Ontario, N2L 3G1, Canada
[b] Department of Civil and Environmental Engineering, University of Waterloo, Waterloo, Ontario, N2L 3G1, Canada
[c] School of Information Engineering, China University of Geosciences, Beijing, 100083, China
[d] Fujian Key Laboratory of Sensing and Computing for Smart Cities, School of Informatics, Xiamen University, Xiamen, FJ, 361005, China
[e] Shaanxi Key Laboratory of Land Consolidation, School of Land Engineering, Chang'an University, Xi'an, Shaanxi, 710064, China
[f] School of Land Engineering, Chang'an University, Xi'an, Shaanxi, 710064, China

A R T I C L E I N F O

Article history:
Received 31 August 2020
Received in revised form
6 March 2021
Accepted 8 March 2021
Available online 9 March 2021

Keywords:
$PM_{2.5}$
Air pollution
Premature mortality
Health impact
Environmental inequality

A B S T R A C T

In the past decade, particulate matter with aerodynamic diameter less than 2.5 μm ($PM_{2.5}$) has reached unprecedented levels in China and posed a significant threat to public health. Exploring the long-term trajectory of the $PM_{2.5}$ attributable health burden and corresponding disparities across populations in China yields insights for policymakers regarding the effectiveness of efforts to reduce air pollution exposure. Therefore, we examine how the magnitude and equity of the $PM_{2.5}$-related public health burden has changed nationally, and between provinces, as economic growth and pollution levels varied during 2005–2017. We derive long-term $PM_{2.5}$ exposures in China from satellite-based observations and chemical transport models, and estimate attributable premature mortality using the Global Exposure Mortality Model (GEMM). We characterize national and interprovincial inequality in health outcomes using environmental Lorenz curves and Gini coefficients over the study period. $PM_{2.5}$ exposure is linked to 1.8 (95% CI: 1.6, 2.0) million premature deaths over China in 2017, increasing by 31% from 2005. Approximately 70% of $PM_{2.5}$ attributable deaths were caused by stroke and IHD (ischemic heart disease), though COPD (chronic obstructive pulmonary disease) and LRI (lower respiratory infection) disproportionately affected poorer provinces. While most economic gains and $PM_{2.5}$-related deaths were concentrated in a few provinces, both gains and deaths became more equitably distributed across provinces over time. As a nation, however, trends toward equality were more recent and less clear cut across causes of death. The rise in premature mortality is due primarily to population growth and baseline risks of stroke and IHD. This rising health burden could be alleviated through policies to prevent pollution, exposure, and disease. More targeted programs may be warranted for poorer provinces with a disproportionate share of $PM_{2.5}$-related premature deaths due to COPD and LRI.

Main findings

The total health burden continues to rise despite lower $PM_{2.5}$ exposures during 2005–2017, but it has become more equitably distributed across provinces in China.

1. Introduction

The adverse impacts of $PM_{2.5}$ (i.e., particulate matter with aerodynamic diameter less than 2.5 μm) on human health are well established. Exposure to ambient $PM_{2.5}$ was associated with an estimated 4.2 million (95% CI: 3.7, 4.8) global premature deaths in 2015 (Cohen et al., 2017). Over 30% of these deaths occurred in China in 2012 (WHO 2016), where ambient $PM_{2.5}$ ranked fourth nationally among 67 risk factors for disability-adjusted life-years (DALYs) (Yang et al., 2013). The most common non-communicable diseases in China are all associated with $PM_{2.5}$ exposure,

☆ This paper has been recommended for acceptance by Dr. Payam Dadvand.

* Corresponding author. Department of Civil and Environmental Engineering, University of Waterloo, Waterloo, Ontario, N2L 3G1, Canada.
E-mail addresses: mingliu@chd.edu.cn (M. Liu), rsaari@uwaterloo.ca (R.K. Saari).

https://doi.org/10.1016/j.envpol.2021.116882
0269-7491/

including chronic obstructive pulmonary disease (COPD), ischemic heart disease (IHD), lung cancer (LC), and stroke (Zhou et al., 2016).

The dramatic rise in $PM_{2.5}$-related mortality in China has coincided with significant economic growth (Liu et al., 2017). In response, the Chinese government has established and updated air quality standards, issued pollution control policies, expanded monitoring networks, and launched targeted initiatives to mitigate air pollution. The policy response began in earnest in 2013 with the Air Pollution Prevention and Control Action Plan (APPCAP) (Huang et al., 2018). Although many studies have examined the effect of such actions on $PM_{2.5}$ concentrations (Ma et al., 2019; Xue et al., 2019a; Yu et al., 2019; Zhang et al., 2020), fewer have quantified the resulting changes in the public health impacts over these important recent decades (Li et al., 2021; Zhao et al., 2018). Many others present national mortality estimates for one or more years, but do not provide a long time-series (see Table S7). Some subnational studies have presented decadal time series of $PM_{2.5}$-related mortality (Lu et al., 2019; Zheng et al., 2015b; Zhu et al., 2019). Few studies present the national mortality burden in China over time (Li et al., 2021; Liu et al., 2017; Xie et al., 2016a). A decadal time series of exposure and its health impacts can inform air quality policies by quantifying changes in the resulting public health burden (Fann et al., 2018). Further, it can be used to evaluate the resulting trends in national and interprovincial equity (Muller et al., 2018).

Changes in the growing Chinese economy and resulting air pollution can impose unequal impacts across the population. Between 2006 and 2017, measures of economic inequality in China peaked shortly after the Great Recession, followed by a shift towards greater equality (Li and Sicular 2014). Air pollution is known to have significant economic impacts in China, for example, resulting in a 5.9% loss in GDP from 1997 to 2005 (Matus et al., 2012). The health and economic burden associated with $PM_{2.5}$ can disproportionately affect vulnerable populations (Bell and Ebisu 2012; Huang et al., 2019; Zhao et al., 2019). The WHO (World Health Organization) (2018) reported that 91% of global premature deaths attributable to air pollution occurred in low- and middle-income countries. Patterns of environmental inequality, typically quantified by metrics such as the Atkinson Index and Gini Index, vary substantially by location (Clark et al., 2014; Fann et al., 2018; Muller et al., 2018; Rosofsky et al., 2018). Policies to reduce air pollution can offer substantial economic benefits; however, some provinces can gain while others lose, which can increase the gap in prosperity between provinces (Xie et al., 2016b). While many studies have examined $PM_{2.5}$–related health impacts in China, to our knowledge, few have explored how these impacts are distributed across regions and income groups (Hajat et al., 2015). Tracking the distribution of $PM_{2.5}$-related health impacts among subpopulations can help to formulate and monitor targeted policies to alleviate inequality.

China's network of air quality monitors has grown since 2013. Methods with more complete spatial coverage are still needed, however, for studying historical air quality and regions with fewer monitors (such as western China). Previous studies of $PM_{2.5}$ concentrations and related premature mortality in China have addressed gaps in ground-level air quality measurements using techniques including artificial intelligence (Li et al., 2019; Xue et al., 2019a), satellite data (Lu et al., 2019; Zheng et al., 2015), chemical transport models (CTMs) (Xie et al., 2016b; 2019), or a combination thereof (Geng et al., 2015; van Donkelaar et al., 2016; Xie et al., 2016a).

Once concentrations are known, concentration-response functions (CRFs) are needed to estimate $PM_{2.5}$-related mortality. CRFs should represent the full potential concentration-response in the underlying population. Ideally, CRFs should be based on local, high-quality observations within the relevant range of concentrations (West et al., 2016). Without CRFs appropriate for high-concentration regions, like China, $PM_{2.5}$-related risks may be underestimated (Maji et al., 2018b; Pope C. Arden et al., 2018). CRFs currently applied in China are mostly derived from lower-concentration regions, like western Europe and North America. One example is the Integrated Exposure-Response (IER) function employed in the Global Burden of Disease (GBD) study (Maji et al., 2018a; Zhao et al., 2018). Yin et al. (2017) reported higher hazard ratio estimates from a national Chinese cohort study than the IER estimates. The Global Exposure Mortality Model (GEMM) introduced by Burnett et al. (2018) also yields higher estimates than the IER. It is based on cohort studies (including one conducted in China) that represent outdoor $PM_{2.5}$ exposure in 97% of the global population. The GEMM can be used to estimate $PM_{2.5}$-related premature mortality across multiple causes of death, including COPD, IHD, LC, lower respiratory infection (LRI), and stroke.

Here, we quantify long-term $PM_{2.5}$ exposures, cause-specific premature mortality and environmental inequality over China. We leverage satellite-based and CTM-driven estimates of exposure, and the GEMM CRF, to estimate $PM_{2.5}$-related premature mortality at a spatial resolution of 3 km. We quantify the corresponding health disparities at the provincial and national levels using a modified Gini coefficient based on mortality. This paper seeks to answer the following questions: (1) How do $PM_{2.5}$ levels and related health burdens vary spatially and temporally over China between 2005 and 2017? (2) How equitably is the $PM_{2.5}$-related health burden distributed across populations in different regions and with different socioeconomic characteristics (i.e. GDP per capita)? (3) How does this pattern of environmental inequality change over the study period?

2. Data and methods

2.1. Ground-level $PM_{2.5}$ observations

Air pollutant measurements in China were released to the public in 2013, providing data to support $PM_{2.5}$ modelling and validation. Here, we use the ground-level $PM_{2.5}$ concentrations (2013–2017) from the China National Environmental Monitoring Center (CNEMC) (http://www.cnemc.cn/). The number of stations available increased over the study period from 519 in 2013 to 1414 in 2017 (detailed in Supplementary Information Section 1.1). The collected hourly measurements were averaged to obtain $PM_{2.5}$ concentrations. Ground-level measurements before 2013 were collected from previous publications (listed in the Supplementary Material Section S1 Table S1). As data before 2013 were limited, these measurements were only used for validation.

2.2. Ground-level $PM_{2.5}$ estimation

Two strategies were used to estimate ground-level $PM_{2.5}$ concentrations over China from 2005 to 2017 using satellite and meteorological data: a previously developed fused dataset (referred to as "fused data" herein) (van Donkelaar et al., 2015, 2019), and a new semi-geographical weighted regression (semi-GWR) model developed herein. The fused data, with a spatial resolution of 0.01°, is used for its superior performance in the years 2005–2012. These surface-level $PM_{2.5}$ concentrations, combining multi-sensor satellite and ground-based AOD, the GEOS-Chem CTM (as a source of AOD and the AOD/$PM_{2.5}$ relationship), and surface monitor observations, are provided by the "Atmospheric Composition Analysis Group" at Dalhousie University (van Donkelaar et al., 2016). Their superior performance in 2005–2012 is attributed to the multiple concentration sources used, which make up for the limited ground-based monitoring data of $PM_{2.5}$ in this period. These fused data have been used in previous environmental and health impact studies (Peng et al., 2016; Sherbinin et al., 2014; Xue et al., 2019b). A detailed description is provided in Supplementary Information Section 2.1.

To obtain $PM_{2.5}$ concentrations between 2013 and 2017, we used published air pollutant measurements from the Chinese government to build and train a semi-GWR model. This type of model accounts for the spatial autocorrelation of variables. The semi-GWR had a better performance than the fused data for the years 2013–2017, especially 2017 (details in Figs. S4–S5). The model structure is provided in Eq. (1):

$$\begin{aligned} PM_{2.5\_GWR(i,j,y)} = {} & \beta_{0(i,j,y)} + \beta_{b_{ext,dry}(i,j,y)} b_{ext,dry\,(i,j,y)} + \beta_{T(i,j,y)} T_{(i,j,y)} \\ & + \beta_{WS(i,j,y)} WS_{(i,j,y)} + \beta_{V(i,j,y)} V_{(i,j,y)} \\ & + \beta_{DEM(i,j,y)} DEM_{(i,j,y)} + \varepsilon_{(i,j,y)} \end{aligned} \tag{1}$$

where $PM_{2.5\_GWR(i,j,y)}$ is the annual ground-level $PM_{2.5}$ concentration at location (i, j) in year y. $b_{ext,dry}$ is extinction coefficient under dry conditions. T, WS, V, and DEM are temperature, wind speed, visibility, and elevation, respectively; these variables were chosen for their influence on surface $PM_{2.5}$, with further details, references, and theory discussed in Supplemental Information Section 1.2. β_0 is the intercept for each year.β denotes the slope of the variable with the corresponding subscript. $\varepsilon_{(i,j,y)}$ is the error term at location (i,j) in year y. The variance inflation factor was calculated to ensure low collinearity of the variables. Geographic weights were estimated with Gaussian distance decay functions ($w_{ij} = \exp(-d_{ij}^2/\theta^2)$, where d is the Euclidean distance between location i and j; θ is the bandwidth size) (Su et al., 2012). All parameters were resampled to 3 km using the cubic convolution resampling algorithm and unified with respect to coordinate systems, data formats, and image sizes. Since the optical-mass relationship has proven to be related to aerosol hygroscopic growth and the height of planetary boundary layer (HPBL) (Kaufman et al., 2003; Koelemeijer et al., 2006), the ground-level extinction coefficient under dry conditions $b_{ext,dry}$ was calculated using satellite-observed AOD (τ) at 550 nm:

$$b_{ext,dry} = \tau \Big/ (HPBL \times f(RH)) \tag{2}$$

where $f(RH)$ is hygroscopic growth coefficient, which was calculated, as in Liu et al. (2019), by geographically weighting three different estimates developed in China (Chen et al., 2014; Liu et al., 2008; Zhang et al., 2015b).

Two concentration estimates (i.e., from the semi-GWR model and the fused concentration data) were validated against ground-level measurements (with details in the Supplementary Information Section 3.1). The semi-GWR model performed better than the fused concentrations from 2013 to 2017, with an average $R^2 = 0.81$ (Fig. S4); however, the model could not be trained before 2013 due to the limited available samples. The fused data offered stable predictive and explanatory power throughout the full study period. They further provided reliable concentration estimates before the monitoring network expanded in 2013, with R^2 equal to 0.65 over the years 2005–2012 (Fig. S5). To unify the spatial distribution and coverage of these two concentration sources, the fused data from 2013 to 2017 were corrected by the GWR-based results using linear regressions to generate the final estimates. The regression coefficients were fitted at the provincial level.

2.3. Health data

Baseline incidence rates were used for the five leading causes of death (COD) associated with $PM_{2.5}$, namely COPD, IHD, LC, LRI, and stroke. They were obtained at the provincial scale from Zhou et al. (2016). The annual variation of mortality rates during the study period in China was generated from the GBD dataset found at http://ghdx.healthdata.org/. The province-level baselines for each year were calculated based on the assumption that the annual variation for each province followed the national trend. Trends of baseline incidence rates by COD are provided in Fig. S1.

2.4. Mortality assessment

Cause-specific premature mortality (ΔM) attributable to $PM_{2.5}$ exposure over China was estimated using Eq. (3).

$$\Delta M = y_0 \times pop \times (RR - 1)/RR \tag{3}$$

where y_0 represents the baseline incidence rate for each COD. pop represents the age-specific population exposed to ambient $PM_{2.5}$. RR represents the corresponding Relative Risk at a given concentration, which was calculated using the GEMM. The GEMM, a set of CRFs established by Burnett et al. (2018), was used here to quantify $PM_{2.5}$ attributable health impacts. The CRFs in the GEMM have several strengths, including a flexible design and comprehensive, high quality input. They vary across the total inhaled dose. They were developed using cohort studies from 16 countries (including a Chinese cohort study), thereby including most of the global population and a wide range of ambient $PM_{2.5}$ concentrations. Relative Risk in the GEMM has the functional form:

$$RR = \exp((\theta \log(1 + \Delta C / \alpha)) / (1 + \exp(-(\Delta C - \mu) / \nu))) \tag{4}$$

where ΔC represents the difference between ambient $PM_{2.5}$ concentrations and the baseline concentration; α, θ, μ, ν define the shape of the CRF (θ and its SE were estimated using the Cox proportional hazards model) (Burnett et al., 2018). GEMM includes forms for pooled cohorts and specific cohorts. The COD-specific RR calculations in this study were based on the age-specific model parameters for the Chinese cohort study, as in Burnett et al. (2018) (provided in Supplemental Material Table S3). A baseline concentration of 2.4 $\mu g/m^3$ was used based on the lowest observed exposure in any cohort. One thousand Monte Carlo simulations were conducted to estimate the 95th confidence interval (CI) in excess premature mortality.

2.5. Socioeconomic data

Gridded population and GDP data in the base years (2005, 2010 and 2015) were obtained from the Resource and Environmental Science Data Center of the Chinese Academy of Sciences (RESDC) (http://www.resdc.cn/) at a spatial resolution of 1 km (Xu 2017). The gridded population and GDP data for the remaining years were calculated by assuming that the proportion of the provincial population and GDP contained in each grid remained constant over the intervening years (i.e., between 2005 and 2009, 2010–2014, and 2015–2017). The province-level annual population, demographic data, and GDP from 2005 to 2017 were from the Chinese National Bureau of Statistics (http://www.stats.gov.cn/tjsj/ndsj/) (see Fig. S1 for (a) population and (b) age distribution). Both gridded population and GDP data were resampled to 3 km to match the spatial resolution of the ground-level $PM_{2.5}$ concentrations. Trends in population and age structure are shown in Figs. S1–S2.

2.6. Inequality analysis

We estimated measures of both economic and environmental inequality. We used the traditional Lorenz curve to characterize the distribution of GDP per capita, which, due to data availability, we used instead of income (Gastwirth and Glauberman 1976). We built on this concept to characterize the distribution of $PM_{2.5}$ attributable premature mortality. To do this, population and excess premature mortality in each pixel were first ranked by GDP per capita. The cumulative share of mortality was then plotted against the cumulative share of population, ranked by GDP per capita (see Fig. S3). We also built Lorenz curves at the provincial scale to evaluate the distribution of mortality between provinces (ranked by provincial GDP per capita) as a measure of interprovincial inequality. Based on the Lorenz curve, the Gini coefficient was calculated by dividing the area of A by 0.5 (which equals to A + B in Fig. S3a). The smaller the Gini coefficient, the smaller the area between the Lorenz curve and the ideal equality line. Thus, a smaller Gini reflects greater equality. The Gini coefficient was calculated as follows:

$$Gini = 1 - \sum_{i=1}^{n} (x_i - x_{i-1})(y_i - y_{i-1}) \tag{5}$$

where n represents the number of pixels/provinces; x_i represents the cumulative percentage of the population in pixel/province i; y_i represents the cumulative percentage of the $PM_{2.5}$-attributable premature deaths (Stroke, COPD, IHD, LC, LRIs). Similar metrics were evaluated for each of the five causes of death (5-COD).

3. Results

3.1. $PM_{2.5}$ exposure assessment

Fig. 1(a) shows the spatial distribution of 13-year mean $PM_{2.5}$ surface concentration estimates and station-based measurements over China. The highest $PM_{2.5}$ concentrations were found in the Taklamakan Desert, where natural particle sources, such as dust and sand, dominate (Huang et al., 2008). The highest exposures, however, were found in major urban areas with high population density (shown in Fig. 1(b)) and high anthropogenic emissions. The Beijing-Tianjin-Hebei (BTH) region, the Sichuan Basin, and central China (including Shanxi, Henan and part of Shandong, Jiangsu, Anhui, and Shaanxi provinces) are examples of dense urban areas with high anthropogenic emissions and high $PM_{2.5}$ concentrations (Zhang et al., 2013; 2015a; Zheng et al., 2015a). The provinces with the highest exposures were Henan and Hebei, with population-weighted mean $PM_{2.5}$ concentrations over the 13-year period exceeding 72 μg/m^3. Maps of geographical annual mean and population-weighted mean $PM_{2.5}$ concentrations for each year are provided in Figs. S6–S7.

Fig. 2(b) shows the time-series of national $PM_{2.5}$ concentrations. It includes national estimated exposure (population-weighted mean concentration; green line), national estimated concentration (geographical mean; yellow line), measured concentration (mean across stations; dashed magenta line) and the equivalent estimated concentration (mean across pixels containing stations; cyan line). Estimated national $PM_{2.5}$ exposure trended downward overall from 2005 to 2017, with a 13-year national mean of 49 μg/m^3. The steepest decrease occurred after 2013, when China issued the Air Pollution Prevention and Control Action Plan (APPCAP), and population-weighted $PM_{2.5}$ concentrations fell by 21% over the next four years. China also began expanding the monitoring network in 2013. It became more representative of population exposure, as shown by the convergence between the national exposure estimates (green line) and the average of concentrations across station-containing pixels (cyan line).

Estimated ground-level concentrations were validated against the annual-mean station-based measurements for each available station, as shown in Fig. 2(a) and Table S5. The overall R^2 was 0.81 and the root mean square error (RMSE) was 8.3 μg/m^3. Fig. 1(a) shows the spatial pattern of estimated concentrations was also consistent with that of ground measurements. These findings, and further validation details provided in Supplemental Results Section 3.1, indicate that the estimated $PM_{2.5}$ concentrations were sufficiently reliable for our analysis.

3.2. Mortality attributable to $PM_{2.5}$

Premature mortality attributable to chronic $PM_{2.5}$ exposure was estimated using equation (3). It was applied to the Chinese population for the years 2005–2017. Excess premature deaths were calculated across five causes of deaths (5-COD), (i.e. COPD, IHD, LC, LRI, and stroke), and shown in Fig. 3. COPD mortality related to $PM_{2.5}$ exposure decreased from 280 (95% CI: 240, 320) thousand in 2005 to 250 (95% CI: 220, 290) thousand in 2017; IHD mortality increased from 390 (95% CI: 370, 400) thousand in 2005 to 680 (95% CI: 660, 690) thousand in 2017, with a peak of 700 (95% CI: 680, 710) thousand in 2015; LC mortality increased from 94 (95% CI: 85, 100) thousand in 2005 to 160 (95% CI: 140, 180) thousand in 2017; LRI mortality decreased from 120 (95% CI: 100, 130) thousand in 2005 to 98 (95% CI: 85, 110) thousand in 2017.

The contribution of each COD to the total cause-specific mortality is shown in Fig. 4. Summed across all five causes of death, the total (or "5-COD") mortality rose from 1.4 (95% CI: 1.2, 1.5) million in 2005 to 1.9 (95% CI: 1.7, 2.1) million in 2015, before dropping to 1.8 (95% CI: 1.6, 2.0) million in 2017. Stroke and IHD were the two leading causes of deaths attributable to $PM_{2.5}$ exposure over China. Over the 13-year period, the annual mean premature deaths associated with stoke and IHD were 580 (95% CI: 510, 660) and 560 (95% CI: 550, 570) thousand deaths, respectively. Together, they comprised 70% of 5-COD mortality, contributing 36% and 34%, respectively. The average number of premature deaths caused by COPD, LC and LRI was 260 (95% CI: 230, 300), 130 (95% CI: 120, 150) and 110 (95% CI: 93, 120) thousand, respectively, which comprised 16%, 8.0% and 6.5% of the total cause-specific mortality during the study period.

Table 1 shows the 13-year (2005–2017) mean annual $PM_{2.5}$ attributable premature mortality by cause of death and by region. Henan, Shandong, Hebei, and Sichuan had the highest mean values (160, 140, 120, and 110 thousand deaths per year, respectively) comprising 33% of the national total. Mortality by IHD and stroke were highest in Henan province, with values of 60 (95% CI: 59, 61) and 67 (95% CI: 59, 74) thousand deaths per year, respectively. $PM_{2.5}$-related mortality caused by COPD and LRIs peaked at 32 (95% CI: 28, 37) and 8.8 (95% CI: 7.8, 9.8) thousand deaths per year in Sichuan province. Shandong province had the highest mean LC mortality.

The spatial distribution of $PM_{2.5}$-attributable premature mortality by cause of death is shown in Fig. 5 and Figs. S9–S13. The mortality hotspots for most CODs shifted from the Sichuan Basin to the Beijing-Tianjin-Hebei region between 2005 and 2017. This might be related to shifting and rising levels of air pollution (Xue et al., 2019a) and population (Li et al., 2021) (Table S6). Mortality incidence rates (in deaths per 100,000 people per year) are provided for the entire study period, for each province and COD, in Figs. S14–S15.

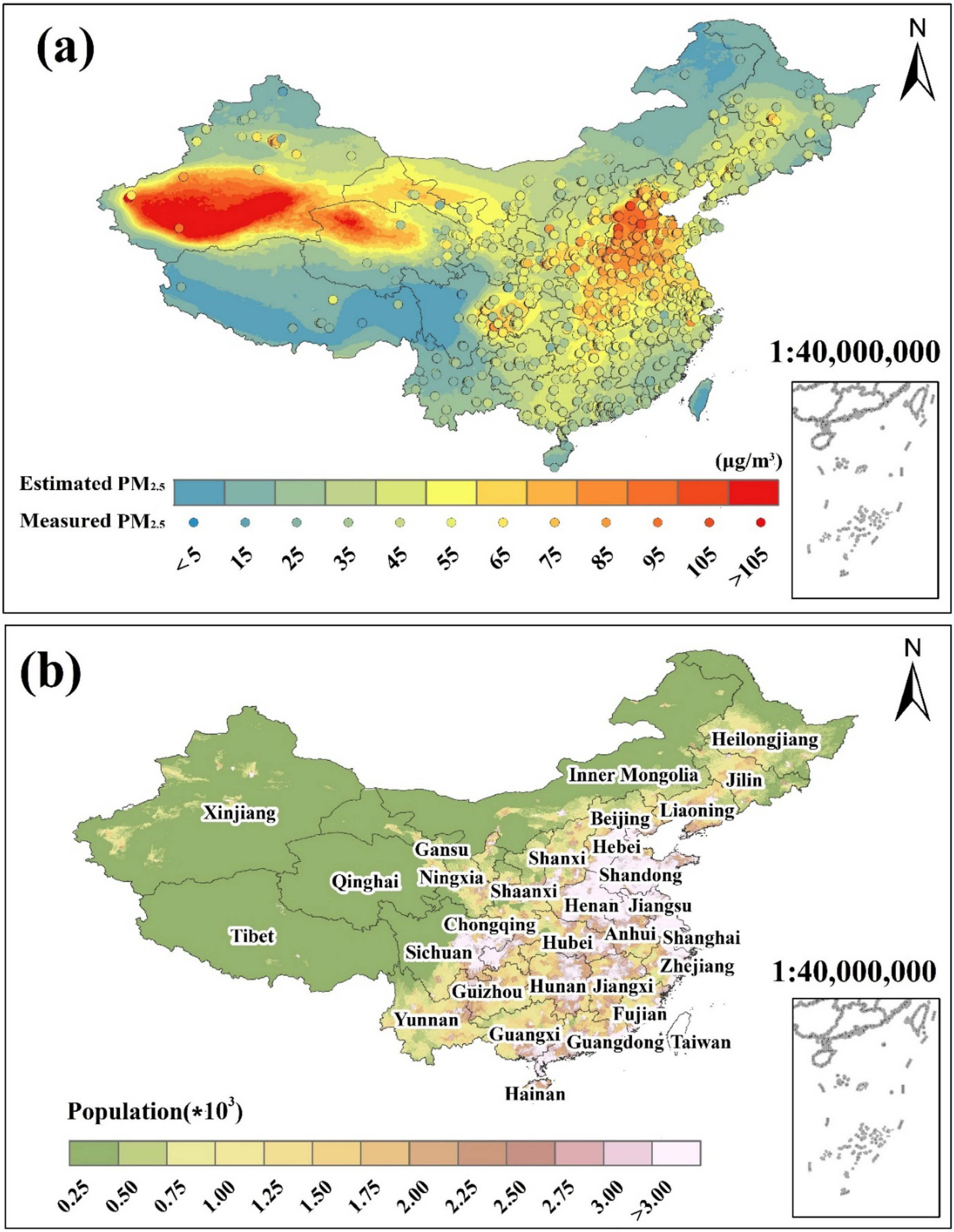

Fig. 1. Spatial distributions of (a) 13-year mean $PM_{2.5}$ concentration estimates and station-based measurements (b) population in 2017 in China.

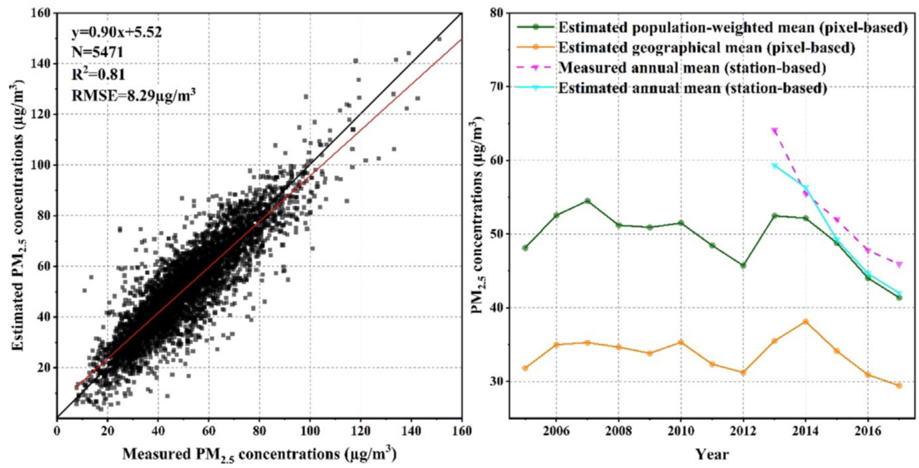

Fig. 2. (a) Validation results and (b) temporal trends of satellite-based $PM_{2.5}$ estimates in China.

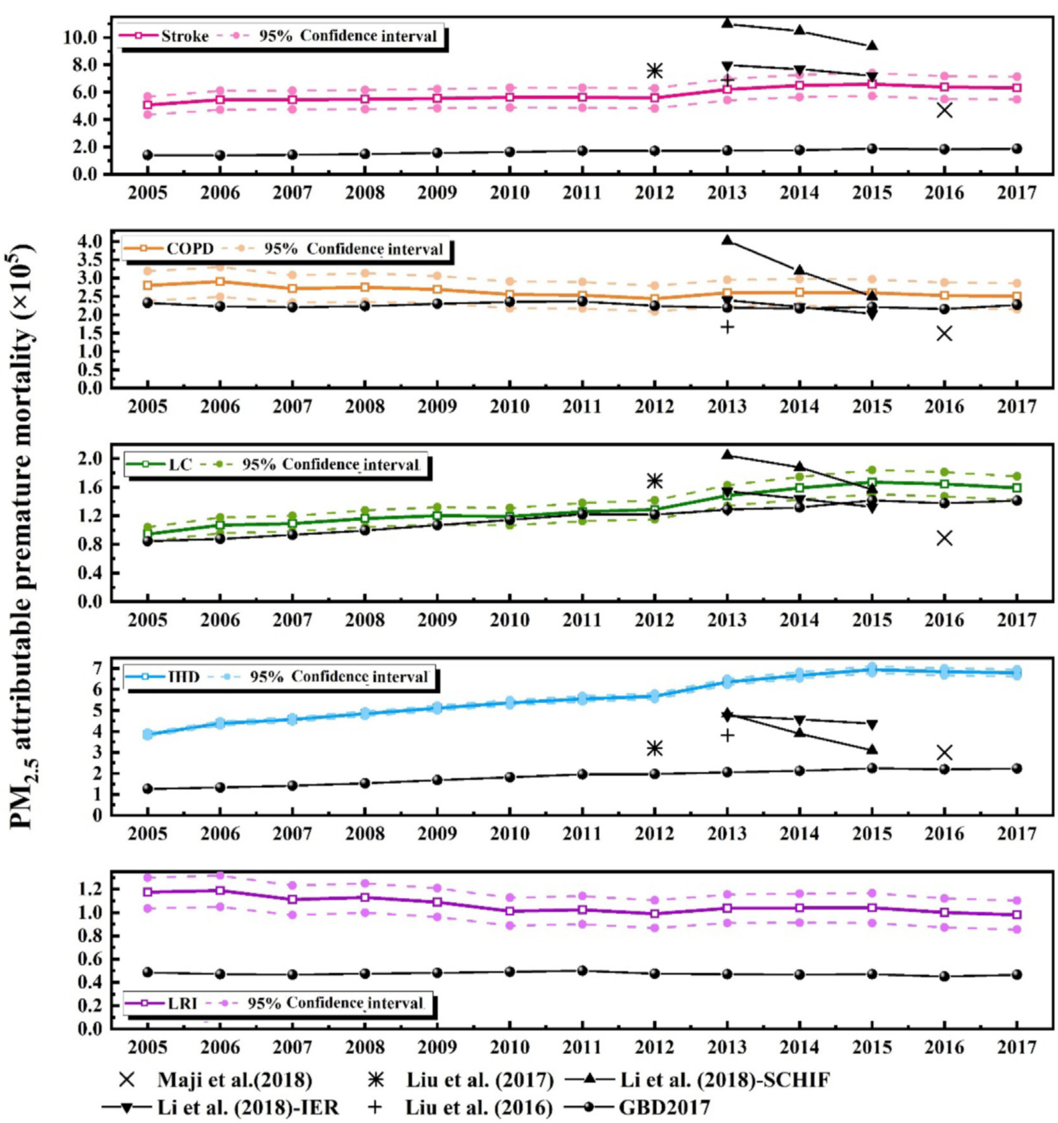

Fig. 3. Temporal trends of disease-specific $PM_{2.5}$ attributable mortality from 2005 to 2017 (median and 95th CI) compared to estimates from previous publications.

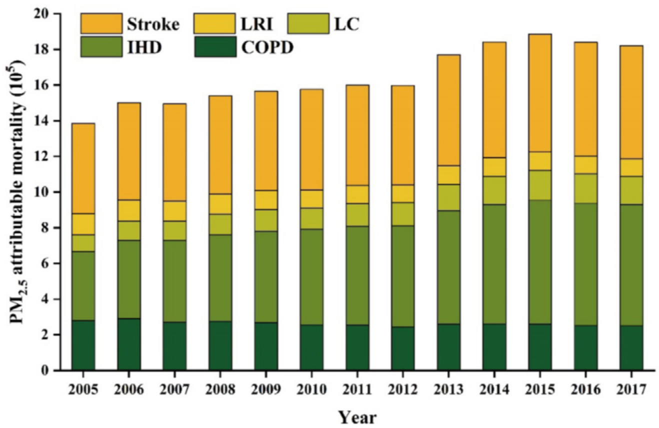

Fig. 4. $PM_{2.5}$ attributable total premature mortality in China by year.

3.3. Inequality analysis

We present multiple metrics of inequality including and expanding on the traditional Gini coefficient. First, we distinguish between traditional economic and health indices. We denote the traditional economic Gini by "GDP per capita". We use GDP per capita as a proxy for income due to data availability. We also calculate a Gini coefficient based on the distribution of deaths by GDP per capita; we denote this coefficient by its respective cause of death on Figs. 6 and 7. Second, we evaluate equity at the national scale, as well as between provinces. We term these metrics as follows: "national Gini" is based on the distribution of GDP per capita across all pixels in the nation; "interprovincial Gini" orders the population in provinces by provincial mean GDP per capita. These national metrics allow us to compare changes in economic and health-related equity over the study period. The interprovincial metrics test whether poorer provinces suffer a disproportionate share of the public health burden from $PM_{2.5}$ pollution.

The national GDP-based Gini (i.e., cyan line) in Fig. 6(a) trends towards greater equality, dropping from approximately 0.42 to 0.31 over the study period. Compared to GDP per capita, $PM_{2.5}$ attributable mortality was more equally distributed. Gini coefficients calculated based on mortality were low, with values less than 0.1. Fig. 6(b) shows that the interprovincial GDP-based Gini similarly declined from 0.27 to 0.20 between 2005 and 2017. Thus, fairness in the distribution of GDP per capita increased both nationally, and among Chinese provinces. A similar decreasing pattern was also observed in the Gini coefficients calculated for COPD, LRI, and stroke. The interprovincial Gini coefficients based on IHD and LC had minuscule mean values of 0.01 and 0.02, respectively.

Fig. 7 shows the Lorenz curves of interprovincial inequality for the years 2005, 2010, 2015, and 2017 (national curves are in the Supplemental Information). As with the mortality-based Gini index (in Fig. 6(b)), the Lorenz curve shows that COPD and LRI disproportionately affected provinces with low GDP per capita. LC mortality was distributed evenly. Low income provinces had proportionately fewer IHD- and stroke-related deaths than middle- to high-income regions.

National total premature mortality was distributed fairly equitably. This is shown by the small 5-COD Gini index in Fig. 6(a), and in the national Lorenz curves (provided in Fig. S16). While the Gini indices of individual CODs were higher, their distributions across GDP per capita balanced each other, resulting in a more equal picture across total premature mortality. Nonetheless, the poor suffered disproportionately. In 2017, the bottom 40th percentile of

Table 1
$PM_{2.5}$ attributable annual premature mortality by COD and province (average of 2005–2017).

Province	COPD (10^3)	IHD (10^3)	LC (10^3)	LRIs (10^3)	Stroke (10^3)	5-COD (10^3)
Anhui	14 (12, 16)	27 (26, 28)	7.5 (6.8, 8.3)	4.7 (4.1, 5.2)	35 (31, 40)	89 (80, 96)
Beijing	2 (1.8, 2.3)	12 (12, 12)	2.6 (2.3, 2.8)	1.8 (1.6, 1.9)	9 (7.9, 10)	27 (25, 29)
Chongqing	11 (9.6, 13)	9.6 (9.3, 9.8)	4 (3.6, 4.4)	2.3 (2, 2.5)	12 (11, 14)	39 (35, 43)
Fujian	4.2 (3.5, 4.8)	6.3 (6.1, 6.5)	1.9 (1.6, 2.1)	2.5 (2.1, 2.8)	6.9 (5.8, 7.9)	22 (19, 24)
Gansu	11 (9.2, 12)	9.8 (9.5, 10)	1.2 (1, 1.3)	2.8 (2.5, 3.2)	9.9 (8.5, 11)	34 (31, 38)
Guangdong	13 (11, 15)	30 (29, 31)	6.6 (5.8, 7.3)	7.6 (6.7, 8.6)	25 (21, 28)	82 (74, 90)
Guangxi	12 (9.9, 13)	19 (18, 19)	4.2 (3.8, 4.7)	7.3 (6.4, 8.1)	18 (15, 20)	60 (54, 66)
Guizhou	12 (10, 14)	9.5 (9.2, 9.7)	2.6 (2.3, 2.8)	6.8 (5.9, 7.6)	17 (15, 19)	48 (42, 53)
Hainan	0.69 (0.58, 0.8)	1.2 (1.2, 1.3)	0.25 (0.22, 0.27)	0.26 (0.22, 0.29)	1.1 (0.9, 1.2)	3.5 (3.1, 3.9)
Hebei	8.6 (7.4, 9.8)	46 (45, 47)	8.9 (8.1, 9.8)	4.9 (4.3, 5.4)	52 (45, 57)	120 (110, 130)
Heilongjiang	3 (2.6, 3.5)	20 (19, 21)	3.6 (3.2, 4)	1.8 (1.6, 2)	13 (11, 15)	41 (38, 45)
Henan	21 (18, 24)	60 (59, 61)	11 (9.8, 12)	6.1 (5.4, 6.7)	67 (59, 74)	160 (150, 180)
Hong Kong	0.02 (0.01, 0.02)	0.05 (0.05, 0.05)	0.01 (0.01, 0.01)	0.02 (0.01, 0.02)	0.03 (0.03, 0.04)	0.13 (0.12, 0.14)
Hubei	14 (12, 16)	26 (25, 26)	6.9 (6.2, 7.6)	3.5 (3.1, 3.9)	33 (29, 37)	84 (76, 91)
Hunan	14 (12, 16)	29 (28, 30)	6.1 (5.5, 6.7)	6.2 (5.5, 6.9)	27 (23, 30)	82 (74, 89)
Inner Mongolia	3.2 (2.8, 3.7)	12 (12, 13)	1.8 (1.6, 2)	1.3 (1.1, 1.4)	9.7 (8.3, 11)	28 (26, 31)
Jiangsu	14 (12, 16)	23 (23, 24)	8.1 (7.3, 8.9)	4 (3.6, 4.5)	33 (29, 37)	83 (75, 90)
Jiangxi	9.2 (7.9, 11)	17 (17, 18)	4.5 (4, 5)	3.1 (2.7, 3.5)	16 (14, 18)	50 (45, 55)
Jilin	1.9 (1.6, 2.2)	15 (15, 16)	2.4 (2.1, 2.6)	1.9 (1.7, 2.1)	11 (9.3, 12)	33 (30, 35)
Liaoning	3.6 (3, 4.1)	22 (21, 22)	5.3 (4.7, 5.8)	3.1 (2.7, 3.5)	19 (16, 21)	53 (48, 57)
Ningxia	1.1 (0.96, 1.3)	3.3 (3.2, 3.3)	0.43 (0.38, 0.48)	0.64 (0.56, 0.71)	2.2 (1.9, 2.5)	7.7 (7, 8.4)
Qinghai	1.8 (1.5, 2)	2.6 (2.5, 2.7)	0.29 (0.26, 0.32)	0.57 (0.5, 0.64)	2.3 (1.9, 2.6)	7.5 (6.7, 8.2)
Shaanxi	5.4 (4.6, 6.1)	19 (18, 19)	2.7 (2.4, 3)	2.5 (2.2, 2.8)	18 (16, 20)	47 (43, 51)
Shandong	18 (16, 20)	55 (53, 56)	14 (12, 15)	5.2 (4.6, 5.8)	52 (45, 57)	140 (130, 150)
Shanghai	2.5 (2.2, 2.9)	3.8 (3.8, 3.9)	1.8 (1.6, 2)	0.46 (0.41, 0.52)	5.1 (4.4, 5.7)	14 (12, 15)
Shanxi	4.9 (4.2, 5.6)	16 (16, 16)	3.4 (3.1, 3.8)	3.1 (2.7, 3.4)	17 (15, 19)	44 (40, 48)
Sichuan	32 (28, 37)	23 (23, 24)	10 (9.2, 11)	8.8 (7.8, 9.8)	35 (30, 39)	110 (98, 120)
Tianjin	1.6 (1.4, 1.8)	10 (10, 11)	2.3 (2.1, 2.5)	1.9 (1.7, 2.1)	7.2 (6.3, 8)	23 (22, 25)
Tibet	0.1 (0.1, 0.1)	0.24 (0.23, 0.25)	0.01 (0.01, 0.01)	0.13 (0.11, 0.15)	0.23 (0.19, 0.27)	0.69 (0.61, 0.77)
Xinjiang	7.3 (6.3, 8.3)	17 (17, 18)	2 (1.8, 2.2)	2.7 (2.4, 3)	12 (11, 14)	41 (38, 45)
Yunnan	7.9 (6.6, 9.1)	9.3 (9, 9.5)	1.8 (1.5, 2)	4.1 (3.5, 4.7)	7.1 (6, 8.3)	30 (27, 34)
Zhejiang	8.1 (6.9, 9.3)	7.5 (7.3, 7.6)	4.5 (4, 4.9)	4.2 (3.7, 4.7)	12 (11, 14)	37 (32, 40)

Note: Numbers in brackets represent 95% CI (2.5th and 97.5th percentile, respectively).

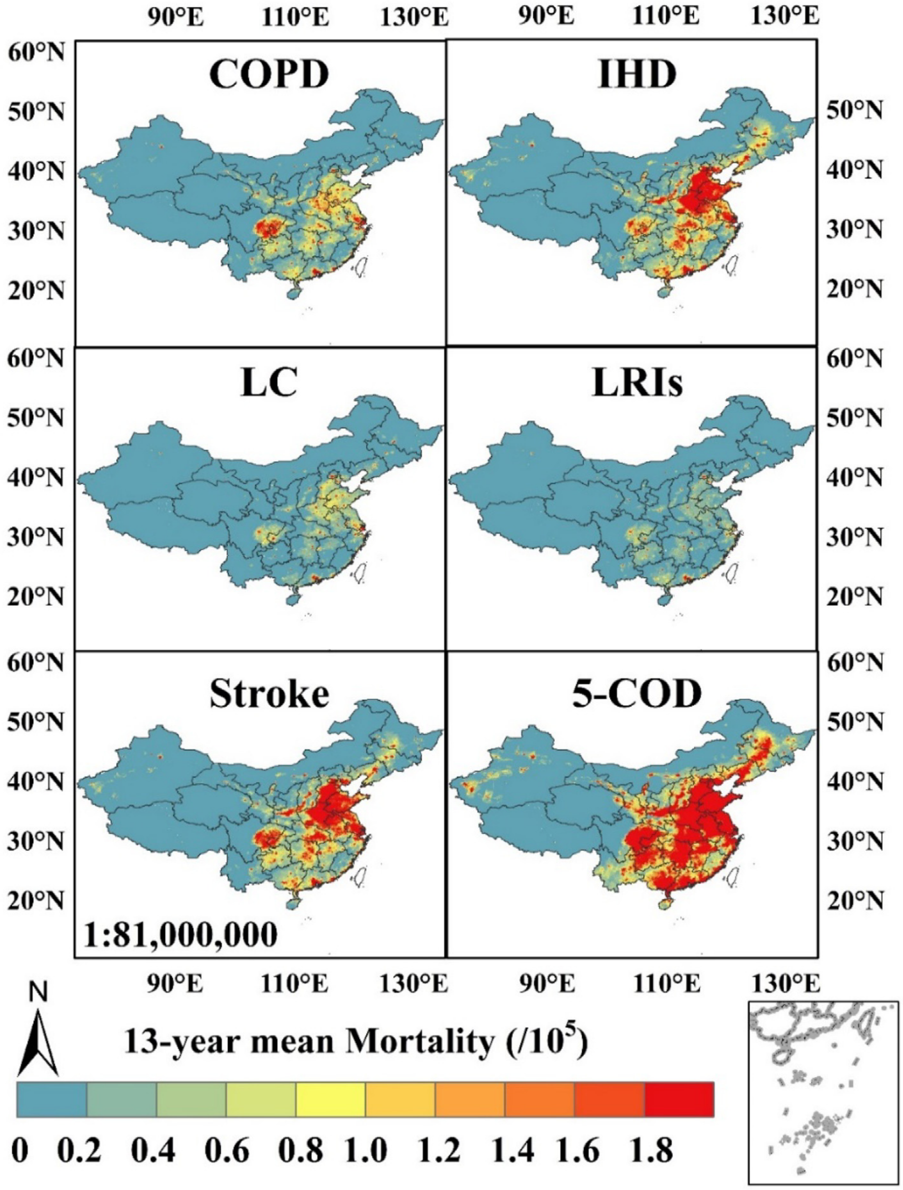

Fig. 5. Spatial patterns of 13-year mean annual $PM_{2.5}$ attributable mortality by cause of death.

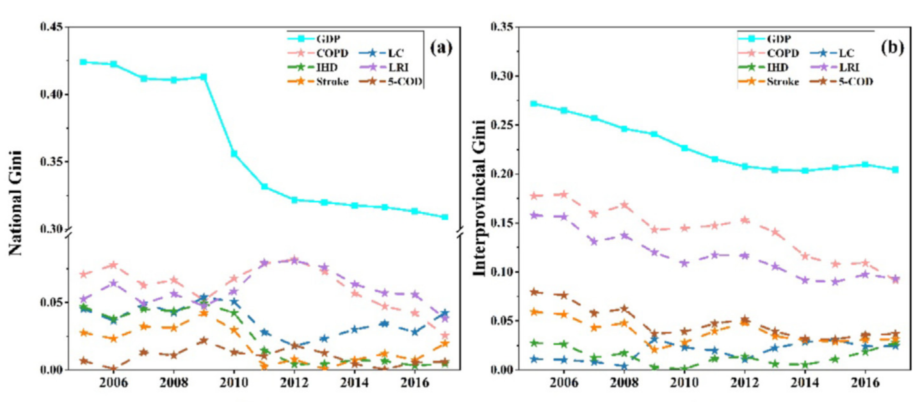

Fig. 6. Temporal trends of (a) national Gini and (b) interprovincial Gini coefficients for GDP per capita and premature mortality caused by different $PM_{2.5}$ related health outcomes.

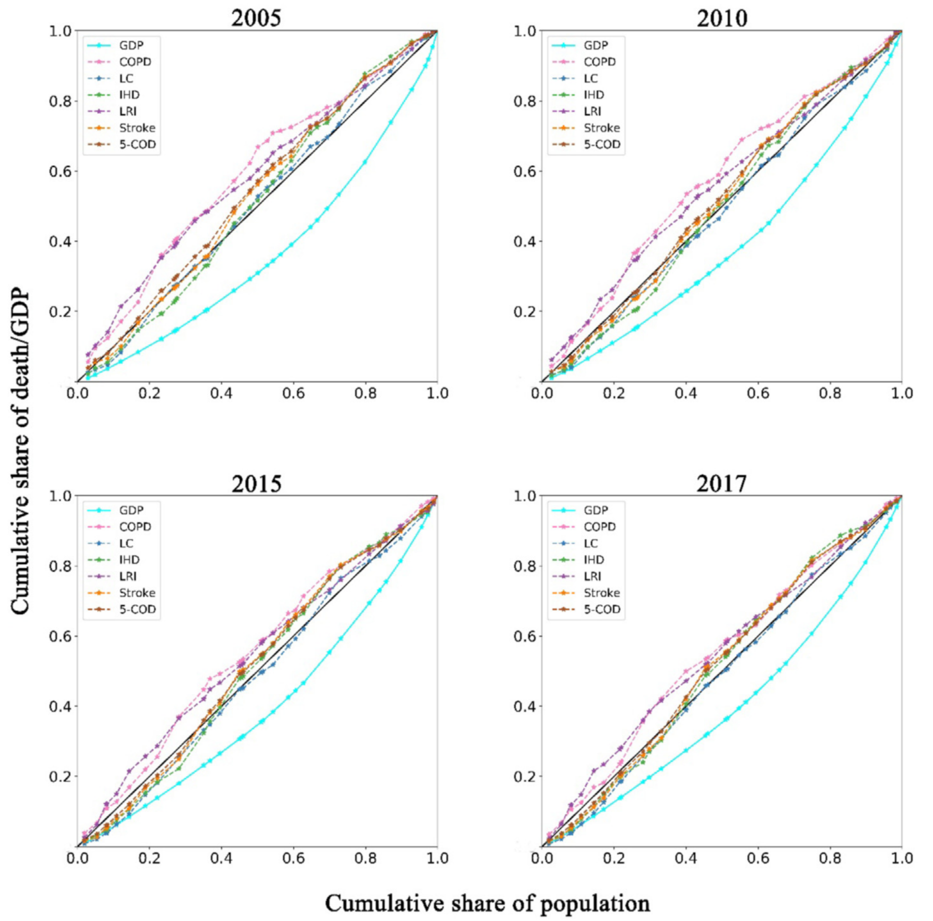

Fig. 7. Interprovincial Lorenz curves for $PM_{2.5}$ attributable premature mortality and economic inequality during 2005–2017.

the Chinese population (sorted by GDP per capita) experienced 43% of $PM_{2.5}$-attributable premature deaths. This translated to an additional 110 (95% CI: 99,120) thousand deaths per year in this group compared to its wealthier counterpart (top 40th percentile sorted by GDP per capita).

4. Discussion

Numerous studies have examined China's air pollution. Fewer have estimated national long-term premature mortality. None, to our knowledge, have quantified the resulting health disparities. Here, we find, as in the GBD-2017 study (Fig. 3), that premature mortality associated with $PM_{2.5}$ continued to rise even after the enactment of significant pollution control policies (i.e., the APPCAP) in 2013. This rise in premature deaths occurred despite concentrations that fell nationally, though concentrations in some provinces rebounded in 2017 (Fig. S8).

Our concentrations compare well with previous studies using long-term national $PM_{2.5}$ for mortality estimation. Compared to other studies with national time-series, our estimates are generally biased low, though are within the 10 $\mu g/m^3$ RMSE of each study (Xiong et al., 2020; Xue et al., 2019a). All three studies show concentrations increasing at the start of the period, then dipping around 2010–2012, rising again, then falling after 2013. Spatially, our 13-year mean concentrations were highest in the Taklamakan Desert in the west, and in urban agglomerations such as those found in the North China Plain and the Sichuan Basin. This pattern is consistent with long-term means found in previous studies. These studies examine an earlier period (Ma et al., 2016; van Donkelaar et al., 2015), a similar period (Xue et al., 2019a), and a longer period (Wei et al., 2021), respectively.

These concentrations resulted in total cause-specific mortality that peaked in 2015, with 1.9 (95% CI: 1.7, 2.1) million annual premature deaths, an increase of 500,000 (or 36%) since 2005. Similar trends were reported in GBD publications. For example, Naghavi et al. (2017) reported that 5-COD mortality rose by 30% from 2005 to 2015 before decreasing to 0.83 million in 2017. While estimates vary widely, total deaths reported here are generally above the means of previous studies (Table S7). Differences between the results of this study and others can be explained by varying $PM_{2.5}$ exposure sources (such as estimation methods, spatial resolution and coverage), CRFs, and other data sources (such as baseline incidence rates and demographics). In particular, by using the GEMM, we expected higher mortality estimates than IER-based studies, since the GEMM RR are larger than those of IER, especially for LRIs, IHD, and stroke (Burnett et al., 2018). Pope C. Arden et al. (2018) pointed out that the IER may underestimate health impacts attributable to $PM_{2.5}$ in highly polluted areas. Here, we used the GEMM CRF based on the Chinese cohort study (Yin et al., 2017) which includes higher pollutant concentrations and yields higher excess risks than the IER (Burnett et al., 2018).

Aside from differences in magnitude, our trends in premature mortality by COD generally match those of the GBD within errors. Over the study period, deaths were generally flat (stroke, COPD), increasing until 2015 then falling (LC, IHD), or decreasing (LRI). Total 5-COD deaths increased over the study period. Xie et al.

(2016a) also shows a similar pattern between its common years (2005 and 2010). Two other national studies, Li et al. (2018) and Li et al. (2021), instead have decreasing trends over 2013–2015 and 2014–2016, respectively. Like these two studies, we also show a decrease in $PM_{2.5}$ concentrations over this period. However, increasing population and baseline rates of most CODs (see Figs. S1–S2) led to an increase in our estimated premature deaths. Li et al. (2021) also show baseline mortality decreasing, which, combined with the decreased exposure, yielded a decrease in deaths. Li et al. (2018) has a higher exposure than other studies in 2013, which could lead to a larger decrease in exposure and overall drop in deaths. Their drop in deaths is small, especially when using IER as opposed to SCHIF. The specific study period also matters. Li et al. (2021) examine 2008–2016, which begins at a relatively high level of $PM_{2.5}$. Thus, their finding a decrease in mortality over this shorter period is not inconsistent with our results. Despite the discrepancies and uncertainties in death estimates across studies, there seems to be clear agreement that deaths have either increased, or, at a minimum, not decreased nearly as steeply as concentrations.

Such $PM_{2.5}$-related premature deaths can disproportionately harm populations of lower socioeconomic status (Hajat et al., 2015). Here, we examined the disparity of mortality incidences across GDP per capita based on differences in ambient concentrations. We place this in the context of economic inequality. At the national scale, China appeared to be trending toward greater economic equality, starting primarily with a steep drop in 2010. This pattern appears to agree with previous studies (Han et al., 2016). It also agrees with national statistics (National Bureau of Statistics), though they show a small recent uptick in the Gini coefficient. Compared to economic inequality, total premature mortality associated with $PM_{2.5}$ was distributed relatively equally across GDP per capita; however, the trend towards equality was not consistent for all causes of death.

We found that COPD and LRI showed the greatest disparity in the distributions of deaths with GDP per capita. This is in line with previous studies showing that COPD-related death has the strongest relationship with socioeconomic status (Pleasants et al., 2016). We found that premature deaths caused by LC and IHD were distributed relatively proportionately across the population, which we attribute to widespread active smoking (Hiscock et al., 2012; Polak et al., 2019; Yusuf et al., 2004). Temporally, interprovincial Ginis for different causes of $PM_{2.5}$-related premature deaths had downward trends. This indicates that $PM_{2.5}$-related mortality risks became more equally distributed between Chinese provinces from 2005 to 2017. Muller et al. (2018) showed a similar pattern among US regions using an adjusted Gini index that accounted for $PM_{2.5}$-related premature mortality. This increasing equality between provinces might be related to the alleviation of air pollution, the economic development of developing provinces, population migration and mobility, and advances in health and education (Liu et al., 2018; Wang et al., 2017).

These findings have several implications for policymakers interested in air pollution and health equity. While policies have reduced ambient pollutant concentrations, the health burden continues to rise. This increasing burden may result from rising baseline risks as well as the growing and aging population. Over this study period, concentrations decreased by 15%, population rose by 8%, and the over-65 age group grew by 26%. Total baseline risks grew by 19%, with IHD in particular rising the most at 53% (see Fig. S1). We leave a quantitative evaluation of these factors to future work. Li et al. (2021) quantified these factors' effect on $PM_{2.5}$-related premature mortality in China over 2008–2016. They ranked changes in concentrations first, followed by population and baseline mortality. While this highlights the need to continue to control exposures, reducing baseline risks also has value. In particular, baseline risks of stroke and IHD are high and growing, which may be related to increased risk factors (such as obesity, hypertension and hypercholesterolemia) (see Fig. S1) (Liu et al., 2011; Ma et al., 2020). Conversely, COPD and LRI have baseline risks which are relatively flat or decreasing. However, these causes of death may disproportionately affect poorer provinces, which could warrant a more targeted intervention to address these health disparities. Any targeted policy to address inequality requires further specific study to account for the effect of a specific intervention using the appropriate metric (Harper et al., 2013).

This study is subject to several limitations. The accuracy of the mortality estimates is limited by uncertainties and spatial resolution of the GEMM and its inputs. Data on baseline mortality could be more precise and comprehensive. Due to data availability, they were obtained and projected at the provincial level based on national trends. This may introduce uncertainty and mask some of the inequality seen in the finer resolution data sources (including $PM_{2.5}$ exposure and GDP per capita). A long-term record of high resolution baseline mortality rates would offer greater accuracy in the magnitude and distribution of excess mortality (Maji et al., 2018b). Uncertainty in $PM_{2.5}$ exposure also affects the health impact assessment. For instance, using concentration sources from two methods may introduce not only bias (resulting from input variables, model structure, and assumptions), but also discontinuities (with differences less than 6.0 $\mu g/m^3$ on average (see Table S8)). However, this strategy was used because it improved the accuracy of $PM_{2.5}$ estimates, especially between 2015 and 2017. We also applied the GEMM Chinese CRF outside of the observed range of concentrations of the Chinese Male Cohort study on which it is based. This may introduce extrapolation errors. Specifically, we observed 13-year mean concentrations exceeding the maximum observed concentration of 83.7 $\mu g/m^3$. Similarly, our counterfactual concentration of 2.4 $\mu g/m^3$ is significantly lower than the minimum observed for the Chinese Male Cohort study (15.4 $\mu g/m^3$). However, evidence from other cohorts, including those in GEMM, suggest that health risks exist at low concentrations. This analysis estimates premature mortality due to outdoor $PM_{2.5}$ exposure, which excludes other $PM_{2.5}$ related exposures, responses, and health impacts. These include, for example, indoor exposure, childhood exposure, differences in individual health effects, other potential causes of death, and morbidity (Lee et al., 2019; Lelieveld et al., 2018; Qi et al., 2017; Steinle et al., 2015). We do not account for $PM_{2.5}$ characteristics (such as chemical composition, size distribution, and sources); nor do we explicitly address the confounding effects of gaseous pollutants co-varying with $PM_{2.5}$ on human health (such as ozone and nitrogen dioxide), which may also bias the mortality estimates in this study (Konishi et al., 2014; Ostro et al., 2015; Pope C. Arden et al., 2018). Our use of GDP per capita based on gridded population is a crude metric for income. Using comprehensive household micro data, including transfers, reveals significant intragroup variability (Rausch et al., 2011). This affects measures of economic inequality, as well as the distributional equity of environmental policies (Rausch et al., 2011). Our work also does not account for the mobility of labour and capital. With significant labour migration between provinces (Luo et al., 2016), there could be some mismatch between the assigned location of exposure, outcome, and income for those who work or die out-of-province. Finally, we likely underestimate the disparity in $PM_{2.5}$-related impacts across GDP per capita. Previous studies suggest that differences in exposure represent a small fraction of the disparity in economic impacts across income groups due to air pollution (Muller et al., 2018; Saari et al., 2017). The characteristics of the exposure, e.g., particulate composition, may be relevant to disparity (Bell and Ebisu 2012). Income, location, and insurance status may affect baseline health status, health care access, outcomes, and economic impacts (Jones et al., 2011; Schoen et al., 2013; Van Ourti et al., 2009; Viscusi and Aldy 2003; Wilper et al., 2009).

5. Conclusion

In recent decades, China saw significant economic development and health risks from air pollution. Here, we examine how equally these impacts were distributed across the nation and between provinces. We present $PM_{2.5}$ exposure, attributable health burdens, and corresponding health disparities over China from 2005 to 2017, with a spatial resolution of 3 km. We find that, though $PM_{2.5}$ exposure declined overall during this period (as seen by comparing population-weighted concentrations at the start (2005) and end (2017) of this period), the number of premature deaths attributable to $PM_{2.5}$ exposure grew. The 5-COD mortality rose from 1.4 (95% CI: 1.2, 1.5) million in 2005 to 1.8 (95% CI: 1.6, 2.0) million in 2017. Stroke and IHD were the two leading causes of death, contributing to approximately 36% and 34% of total cause-specific mortality during 2005–2017, respectively. These two causes dominated due to their prevalence in the population. Their burden could be alleviated not only through environmental policy to further reduce air pollution, but also through broader programs for prevention and treatment of such public health risks. More targeted programs may be warranted for poorer provinces (based on low GDP per capita), as they endured a disproportionate share of $PM_{2.5}$-related premature deaths due to COPD and LRI. Between provinces, the total 5-COD excess premature mortality appeared equally distributed (with Gini coefficients less than 0.1). Nationally, total premature mortality associated with $PM_{2.5}$ was distributed relatively equally by GDP per capita. National measures of equality were steady or became more equitable over time. These findings are based on differences in ambient concentrations, which do not reflect all differences in exposure, baseline health risks, vulnerability, or access to care, all of which could contribute to inequality. Distributional implications should be evaluated in full prior to implementing new interventions to address this public health burden and its resulting health disparities.

Declaration of competing interest

The authors declare that they have no known competing financial interests or personal relationships that could have appeared to influence the work reported in this paper.

Acknowledgements

The first author acknowledges the China Scholarship Council for their support via a doctoral scholarship (No. 201706400072). Rebecca K. Saari acknowledges funding by the Natural Sciences and Engineering Research Council of Canada RPGIN-2016-04132.

Appendix A. Supplementary data

Supplementary data to this article can be found online at https://doi.org/10.1016/j.envpol.2021.116882.

Author statement

Ming Liu: Conceptualization; Methodology; Software; Investigation; Writing – original draft. Rebecca K. Saari.: Supervision; Conceptualization; Writing - Reviewing and Editing. Gaoxiang Zhou: Software; Investigation. Jonathan Li: Supervision; Writing – review & editing. Ling Han: Writing – review & editing. Xiangnan Liu: Writing – review & editing.

References

Arden, Pope C., Cohen Aaron, J., Burnett Richard, T., 2018. Cardiovascular disease and fine particulate matter. Circ. Res. 122, 1645–1647. https://doi.org/10.1161/CIRCRESAHA.118.312956.

Bell, M.L., Ebisu, K., 2012. Environmental inequality in exposures to airborne particulate matter components in the United States. Environ. Health Perspect. 120, 1699–1704. https://doi.org/10.1289/ehp.1205201.

Burnett, R., Chen, H., Szyszkowicz, M., Fann, N., Hubbell, B., Pope, C.A., et al., 2018. Global estimates of mortality associated with long-term exposure to outdoor fine particulate matter. Proc. Natl. Acad. Sci. Unit. States Am. 115, 9592–9597. https://doi.org/10.1073/pnas.1803222115.

Chen, J., Zhao, C.S., Ma, N., Yan, P., 2014. Aerosol hygroscopicity parameter derived from the light scattering enhancement factor measurements in the North China Plain. Atmos. Chem. Phys. 14, 8105–8118. https://doi.org/10.5194/acp-14-8105-2014.

Clark, L.P., Millet, D.B., Marshall, J.D., 2014. National patterns in environmental injustice and inequality: outdoor NO2 air pollution in the United States. In: Zhang, Y. (Ed.), PloS One 9, e94431. https://doi.org/10.1371/journal.pone.0094431.

Cohen, A.J., Brauer, M., Burnett, R., Anderson, H.R., Frostad, J., Estep, K., et al., 2017. Estimates and 25-year trends of the global burden of disease attributable to ambient air pollution: an analysis of data from the Global Burden of Diseases Study 2015. Lancet 389, 1907–1918. https://doi.org/10.1016/S0140-6736(17)30505-6.

Fann, N., Coffman, E., Timin, B., Kelly, J.T., 2018. The estimated change in the level and distribution of $PM_{2.5}$-attributable health impacts in the United States: 2005–2014. Environ. Res. 167, 506–514. https://doi.org/10.1016/j.envres.2018.08.018.

Gastwirth, J.L., Glauberman, M., 1976. The interpolation of the Lorenz curve and Gini index from grouped data. Econometrica 44, 479–483. https://doi.org/10.2307/1913977.

Geng, G., Zhang, Q., Martin, R.V., van Donkelaar, A., Huo, H., Che, H., et al., 2015. Estimating long-term $PM_{2.5}$ concentrations in China using satellite-based aerosol optical depth and a chemical transport model. Rem. Sens. Environ. 166, 262–270. https://doi.org/10.1016/j.rse.2015.05.016.

Hajat, A., Hsia, C., O'Neill, M.S., 2015. Socioeconomic disparities and air pollution exposure: a global review. Current Environmental Health Reports 2, 440–450. https://doi.org/10.1007/s40572-015-0069-5.

Han, J., Zhao, Q., Zhang, M., 2016. China's income inequality in the global context. Perspectives in Science 7, 24–29. https://doi.org/10.1016/j.pisc.2015.11.006.

Harper, S., Ruder, E., Roman, H.A., Geggel, A., Nweke, O., Payne-Sturges, D., et al., 2013. Using inequality measures to incorporate environmental justice into regulatory analyses. Int. J. Environ. Res. Publ. Health 10, 4039–4059. https://doi.org/10.3390/ijerph10094039.

Hiscock, R., Bauld, L., Amos, A., Fidler, J.A., Munafò, M., 2012. Socioeconomic status and smoking: a review. Ann. N. Y. Acad. Sci. 1248, 107–123. https://doi.org/10.1111/j.1749-6632.2011.06202.x.

Huang, J., Minnis, P., Chen, B., Huang, Z., Liu, Z., Zhao, Q., et al., 2008. Long-range transport and vertical structure of Asian dust from CALIPSO and surface measurements during PACDEX. J. Geophys. Res.: Atmosphere 113. https://doi.org/10.1029/2008JD010620.

Huang, G., Zhou, W., Qian, Y., Fisher, B., 2019. Breathing the same air? Socioeconomic disparities in $PM_{2.5}$ exposure and the potential benefits from air filtration. Sci. Total Environ. 657, 619–626. https://doi.org/10.1016/j.scitotenv.2018.11.428.

Jones, A.M., Rice, N., Robone, S., Dias, P.R., 2011. Inequality and polarisation in health systems' responsiveness: a cross-country analysis. J. Health Econ. 30, 616–625. https://doi.org/10.1016/j.jhealeco.2011.05.003.

Kaufman, Y.J., Haywood, J.M., Hobbs, P.V., Hart, W., Kleidman, R., Schmid, B., 2003. Remote sensing of vertical distributions of smoke aerosol off the coast of Africa. Geophys. Res. Lett. 30 https://doi.org/10.1029/2003GL017068.

Koelemeijer, R.B.A., Homan, C.D., Matthijsen, J., 2006. Comparison of spatial and temporal variations of aerosol optical thickness and particulate matter over Europe. Atmos. Environ. 40, 5304–5315. https://doi.org/10.1016/j.atmosenv.2006.04.044.

Konishi, S., Ng, C.F.S., Stickley, A., Nishihata, S., Shinsugi, C., Ueda, K., et al., 2014. Particulate matter modifies the association between airborne pollen and daily medical consultations for pollinosis in Tokyo. Sci. Total Environ. 499, 125–132. https://doi.org/10.1016/j.scitotenv.2014.08.045.

Lee, M., Schwartz, J., Wang, Y., Dominici, F., Zanobetti, A., 2019. Long-term effect of fine particulate matter on hospitalization with dementia. Environ. Pollut. 254, 112926. https://doi.org/10.1016/j.envpol.2019.07.094.

Lelieveld, J., Haines, A., Pozzer, A., 2018. Age-dependent health risk from ambient air pollution: a modelling and data analysis of childhood mortality in middle-income and low-income countries. The Lancet Planetary Health 2, e292–e300. https://doi.org/10.1016/S2542-5196(18)30147-5.

Li, S., Sicular, T., 2014. The distribution of household income in China: inequality, poverty and policies*. China Q. 217, 1–41. https://doi.org/10.1017/S0305741014000290.

Li, J., Liu, H., Lv, Z., Zhao, R., Deng, F., Wang, C., et al., 2018. Estimation of $PM_{2.5}$ mortality burden in China with new exposure estimation and local concentration-response function. Environ. Pollut. 243, 1710–1718. https://doi.org/10.1016/j.envpol.2018.09.089.

Li, J., Han, X., Jin, M., Zhang, X., Wang, S., 2019. Globally analysing spatiotemporal trends of anthropogenic PM2.5 concentration and population's PM2.5 exposure from 1998 to 2016. Environ. Int. 128, 46–62. https://doi.org/10.1016/j.envint.2019.04.026.

Li, Y., Liao, Q., Zhao, X., Tao, Y., Bai, Y., Peng, L., 2021. Premature mortality attributable to $PM_{2.5}$ pollution in China during 2008–2016: underlying causes and responses to emission reductions. Chemosphere 263, 127925. https://doi.org/10.1016/j.chemosphere.2020.127925.

Liu, X., Cheng, Y., Zhang, Y., Jung, J., Sugimoto, N., Chang, S.-Y., et al., 2008. Influences of relative humidity and particle chemical composition on aerosol scattering properties during the 2006 PRD campaign. Atmos. Environ. 42, 1525–1536. https://doi.org/10.1016/j.atmosenv.2007.10.077.

Liu, L., Wang, D., Wong, K.S.L., Wang, Y., 2011. Stroke and stroke care in China: huge burden, significant workload, and a national priority. Stroke 42, 3651–3654. https://doi.org/10.1161/STROKEAHA.111.635755.

Liu, M., Huang, Y., Ma, Z., Jin, Z., Liu, X., Wang, H., et al., 2017. Spatial and temporal trends in the mortality burden of air pollution in China: 2004–2012. Environ. Int. 98, 75–81. https://doi.org/10.1016/j.envint.2016.10.003.

Liu, T., Cai, Y.Y., Feng, B.X., Cao, G.X., Lin, H.L., Xiao, J.P., et al., 2018. Long-term mortality benefits of air quality improvement during the twelfth five-year-plan period in 31 provincial capital cities of China. Atmos. Environ. 173, 53–61. https://doi.org/10.1016/j.atmosenv.2017.10.054.

Liu, M., Zhou, G., Saari, R.K., Li, S., Liu, X., Li, J., 2019. Quantifying $PM_{2.5}$ mass concentration and particle radius using satellite data and an optical-mass conversion algorithm. ISPRS J. Photogrammetry Remote Sens. 158, 90–98. https://doi.org/10.1016/j.isprsjprs.2019.10.010.

Lu, X., Lin, C., Li, W., Chen, Y., Huang, Y., Fung, J.C.H., et al., 2019. Analysis of the adverse health effects of $PM_{2.5}$ from 2001 to 2017 in China and the role of urbanization in aggravating the health burden. Sci. Total Environ. 652, 683–695. https://doi.org/10.1016/j.scitotenv.2018.10.140.

Luo, X., Caron, J., Karplus, V.J., Zhang, D., Zhang, X., 2016. Interprovincial migration and the stringency of energy policy in China. Energy Econ. 58, 164–173. https://doi.org/10.1016/j.eneco.2016.05.017.

Ma, Z., Hu, X., Sayer, A.M., Levy, R., Zhang, Q., Xue, Y., et al., 2016. Satellite-based spatiotemporal trends in $PM_{2.5}$ concentrations: China, 2004-2013. Environ. Health Perspect. 124, 184–192. https://doi.org/10.1289/ehp.1409481.

Ma, Z., Liu, R., Liu, Y., Bi, J., 2019. Effects of air pollution control policies on $PM_{2.5}$ pollution improvement in China from 2005 to 2017: a satellite-based perspective. Atmos. Chem. Phys. 19, 6861–6877. https://doi.org/10.5194/acp-19-6861-2019.

Ma, L.-Y., Chen, W.-W., Gao, R.-L., Liu, L.-S., Zhu, M.-L., Wang, Y.-J., et al., 2020. China cardiovascular diseases report 2018: an updated summary. Journal of Geriatric Cardiology 17, 1–8. https://doi.org/10.11909/j.issn.1671-5411.2020.01.001.

Maji, K.J., Dikshit, A.K., Arora, M., Deshpande, A., 2018a. Estimating premature mortality attributable to $PM_{2.5}$ exposure and benefit of air pollution control policies in China for 2020. Sci. Total Environ. 612, 683–693. https://doi.org/10.1016/j.scitotenv.2017.08.254.

Maji, K.J., Ye, W.-F., Arora, M., Shiva Nagendra, S.M., 2018b. $PM_{2.5}$-related health and economic loss assessment for 338 Chinese cities. Environ. Int. 121, 392–403. https://doi.org/10.1016/j.envint.2018.09.024.

Matus, K., Nam, K.-M., Selin, N.E., Lamsal, L.N., Reilly, J.M., Paltsev, S., 2012. Health damages from air pollution in China. Global Environ. Change 22, 55–66. https://doi.org/10.1016/j.gloenvcha.2011.08.006.

Muller, N.Z., Matthews, P.H., Wiltshire-Gordon, V., 2018. The distribution of income is worse than you think: including pollution impacts into measures of income inequality. J. Balaguer, ed PLoS ONE 13, e0192461. https://doi.org/10.1371/journal.pone.0192461.

Naghavi, M., Abajobir, A.A., Abbafati, C., Abbas, K.M., Abd-Allah, F., Abera, S.F., et al., 2017. Global, regional, and national age-sex specific mortality for 264 causes of death, 1980–2016: a systematic analysis for the Global Burden of Disease Study 2016. Lancet 390, 1151–1210. https://doi.org/10.1016/s0140-6736(17)32152-9.

Ostro, B., Hu, J., Goldberg, D., Reynolds, P., Hertz, A., Bernstein, L., et al., 2015. Associations of mortality with long-term exposures to fine and ultrafine particles, species and sources: results from the California Teachers Study Cohort. Environ. Health Perspect. 123, 549–556. https://doi.org/10.1289/ehp.1408565.

Peng, J., Chen, S., Lü, H., Liu, Y., Wu, J., 2016. Spatiotemporal patterns of remotely sensed $PM_{2.5}$ concentration in China from 1999 to 2011. Rem. Sens. Environ. 174, 109–121. https://doi.org/10.1016/j.rse.2015.12.008.

Pleasants, R.A., Riley, I.L., Mannino, D.M., 2016. Defining and targeting health disparities in chronic obstructive pulmonary disease. Int. J. Chronic Obstr. Pulm. Dis. 11, 2475–2496. https://doi.org/10.2147/COPD.S79077.

Polak, M., Genowska, A., Szafraniec, K., Fryc, J., Jamiołkowski, J., Pająk, A., 2019. Area-based socio-economic inequalities in mortality from lung cancer and respiratory diseases. Int. J. Environ. Res. Publ. Health 16, 1791. https://doi.org/10.3390/ijerph16101791.

Qi, M., Zhu, X., Du, W., Chen, Y., Chen, Y., Huang, T., et al., 2017. Exposure and health impact evaluation based on simultaneous measurement of indoor and ambient $PM_{2.5}$ in Haidian, Beijing. Environ. Pollut. 220, 704–712. https://doi.org/10.1016/j.envpol.2016.10.035.

Rausch, S., Metcalf, G.E., Reilly, J.M., 2011. Distributional impacts of carbon pricing: a general equilibrium approach with micro-data for households. Energy Econ. 33, S20–S33. https://doi.org/10.1016/j.eneco.2011.07.023.

Rosofsky, A., Levy, J.I., Zanobetti, A., Janulewicz, P., Fabian, M.P., 2018. Temporal trends in air pollution exposure inequality in Massachusetts. Environ. Res. 161, 76–86. https://doi.org/10.1016/j.envres.2017.10.028.

Saari, R.K., Thompson, T.M., Selin, N.E., 2017. Human health and economic impacts of ozone reductions by income group. Environ. Sci. Technol. 51, 1953–1961. https://doi.org/10.1021/acs.est.6b04708.

Schoen, C., Radley, D.C., Riley, P., Lippa, J.A., Berenson, J., Dermody, C., Shih, A., 2013. Health care in the two americas: findings from the scorecard on state health system performance for low-income populations. http://www.commonwealthfund.org/publications/fund-reports/2013/sep/low-income-scorecard. (Accessed 21 April 2015).

Sherbinin, A de, Levy, M.A., Zell, E., Weber, S., Jaiteh, M., 2014. Using satellite data to develop environmental indicators. Environ. Res. Lett. 9, 084013 https://doi.org/10.1088/1748-9326/9/8/084013.

Steinle, S., Reis, S., Sabel, C.E., Semple, S., Twigg, M.M., Braban, C.F., et al., 2015. Personal exposure monitoring of $PM_{2.5}$ in indoor and outdoor microenvironments. Sci. Total Environ. 508, 383–394. https://doi.org/10.1016/j.scitotenv.2014.12.003.

Su, S., Xiao, R., Zhang, Y., 2012. Multi-scale analysis of spatially varying relationships between agricultural landscape patterns and urbanization using geographically weighted regression. Appl. Geogr. 32, 360–375. https://doi.org/10.1016/j.apgeog.2011.06.005.

van Donkelaar, A., Martin, R.V., Brauer, M., Boys, B.L., 2015. Use of satellite observations for long-term exposure assessment of global concentrations of fine particulate matter. Environ. Health Perspect. 123, 135–143. https://doi.org/10.1289/ehp.1408646.

van Donkelaar, A., Martin, R.V., Brauer, M., Hsu, N.C., Kahn, R.A., Levy, R.C., et al., 2016. Global estimates of fine particulate matter using a combined geophysical-statistical method with information from satellites, models, and monitors. Environ. Sci. Technol. 50, 3762–3772. https://doi.org/10.1021/acs.est.5b05833.

van Donkelaar, A., Martin, R.V., Li, C., Burnett, R.T., 2019. Regional estimates of chemical composition of fine particulate matter using a combined geoscience-statistical method with information from satellites, models, and monitors. Environ. Sci. Technol. 53, 2595–2611. https://doi.org/10.1021/acs.est.8b06392.

Van Ourti, T., van Doorslaer, E., Koolman, X., 2009. The effect of income growth and inequality on health inequality: theory and empirical evidence from the European Panel. J. Health Econ. 28, 525–539. https://doi.org/10.1016/j.jhealeco.2008.12.005.

Viscusi, W.K., Aldy, J.E., 2003. The value of a statistical life: a critical review of market estimates throughout the world. J. Risk Uncertain. 27, 5–76. https://doi.org/10.1023/A:1025598106257.

Wang, H., Zhang, Y., Zhao, H., Lu, X., Zhang, Y., Zhu, W., et al., 2017. Trade-driven relocation of air pollution and health impacts in China. Nat. Commun. 8, 738. https://doi.org/10.1038/s41467-017-00918-5.

Wei, J., Li, Z., Lyapustin, A., Sun, L., Peng, Y., Xue, W., et al., 2021. Reconstructing 1-km-resolution high-quality $PM_{2.5}$ data records from 2000 to 2018 in China: spatiotemporal variations and policy implications. Rem. Sens. Environ. 252, 112136. https://doi.org/10.1016/j.rse.2020.112136.

West, J.J., Cohen, A., Dentener, F., Brunekreef, B., Zhu, T., Armstrong, B., et al., 2016. What we breathe impacts our health: improving understanding of the link between air pollution and health. Environ. Sci. Technol. 50, 4895–4904. https://doi.org/10.1021/acs.est.5b03827.

WHO, 2016. Ambient Air Pollution: A Global Assessment of Exposure and Burden of Disease.

WHO (World Health Organization), 2018. Ambient (outdoor) air pollution. https://www.who.int/news-room/fact-sheets/detail/ambient-(outdoor)-air-quality-and-health. (Accessed 9 January 2020).

Wilper, A.P., Woolhandler, S., Lasser, K.E., McCormick, D., Bor, D.H., Himmelstein, D.U., 2009. Health insurance and mortality in US adults. Am. J. Publ. Health 99, 2289–2295. https://doi.org/10.2105/AJPH.2008.157685.

Xie, R., Sabel, C.E., Lu, X., Zhu, W., Kan, H., Nielsen, C.P., et al., 2016a. Long-term trend and spatial pattern of $PM_{2.5}$ induced premature mortality in China. Environ. Int. 97, 180–186. https://doi.org/10.1016/j.envint.2016.09.003.

Xie, Y., Dai, H., Dong, H., Hanaoka, T., Masui, T., 2016b. Economic impacts from $PM_{2.5}$ pollution-related health effects in China: a provincial-level analysis. Environ. Sci. Technol. 50, 4836–4843. https://doi.org/10.1021/acs.est.5b05576.

Xie, Y., Dai, H., Zhang, Y., Wu, Y., Hanaoka, T., Masui, T., 2019. Comparison of health and economic impacts of $PM_{2.5}$ and ozone pollution in China. Environ. Int. 130, 104881. https://doi.org/10.1016/j.envint.2019.05.075.

Xiong, H., Lan, L., Liang, L., Liu, Y., Xu, X., 2020. Spatiotemporal differences and dynamic evolution of $PM_{2.5}$ pollution in China. Sustainability 12, 5349. https://doi.org/10.3390/su12135349.

Xu, X., 2017. 1 KM Grid Population Dataset of China. https://doi.org/10.12078/2017121101.

Xue, T., Zheng, Y., Tong, D., Zheng, B., Li, X., Zhu, T., et al., 2019a. Spatiotemporal continuous estimates of $PM_{2.5}$ concentrations in China, 2000–2016: a machine learning method with inputs from satellites, chemical transport model, and ground observations. Environ. Int. 123, 345–357. https://doi.org/10.1016/j.envint.2018.11.075.

Xue, T., Zhu, T., Zheng, Y., Liu, J., Li, X., Zhang, Q., 2019b. Change in the number of $PM_{2.5}$-attributed deaths in China from 2000 to 2010: comparison between estimations from census-based epidemiology and pre-established exposure-response functions. Environ. Int. 129, 430–437. https://doi.org/10.1016/j.envint.2019.05.067.

Yang, G., Wang, Y., Zeng, Y., Gao, G.F., Liang, X., Zhou, M., et al., 2013. Rapid health transition in China, 1990–2010: findings from the global burden of disease study 2010. Lancet 381, 1987–2015. https://doi.org/10.1016/S0140-6736(13)61097-1.

Yin, P., Brauer, M., Cohen, A., Burnett, R., Liu, J., Liu, Y., et al., 2017. Long-term fine particulate matter exposure and nonaccidental and cause-specific mortality in a large national cohort of Chinese men. Environ. Health Perspect. 125, 117002. https://doi.org/10.1289/EHP1673.

Yu, M., Zhu, Y., Lin, C.-J., Wang, S., Xing, J., Jang, C., et al., 2019. Effects of air pollution control measures on air quality improvement in Guangzhou, China. J. Environ. Manag. 244, 127–137. https://doi.org/10.1016/j.jenvman.2019.05.046.

Yusuf, S., Hawken, S., Ôunpuu, S., Dans, T., Avezum, A., Lanas, F., et al., 2004. Effect of potentially modifiable risk factors associated with myocardial infarction in 52 countries (the INTERHEART study): case-control study. Lancet 364, 937–952. https://doi.org/10.1016/S0140-6736(04)17018-9.

Zhang, R., Jing, J., Tao, J., Hsu, S.-C., Wang, G., Cao, J., et al., 2013. Chemical characterization and source apportionment of $PM_{2.5}$ in Beijing: seasonal perspective. Atmos. Chem. Phys. 13, 7053–7074. https://doi.org/10.5194/acp-13-7053-2013.

Zhang, L., Liu, L., Zhao, Y., Gong, S., Zhang, X., Henze, D.K., et al., 2015a. Source attribution of particulate matter pollution over North China with the adjoint method. Environ. Res. Lett. 10, 084011 https://doi.org/10.1088/1748-9326/10/8/084011.

Zhang, L., Sun, J.Y., Shen, X.J., Zhang, Y.M., Che, H., Ma, Q.L., et al., 2015b. Observations of relative humidity effects on aerosol light scattering in the Yangtze River Delta of China. Atmos. Chem. Phys. 15, 8439–8454. https://doi.org/10.5194/acp-15-8439-2015.

Zhang, X., Fung, J.C.H., Zhang, Y., Lau, A.K.H., Leung, K.K.M., Huang, W (Wayne), 2020. Assessing $PM_{2.5}$ emissions in 2020: the impacts of integrated emission control policies in China. Environ. Pollut. 263, 114575. https://doi.org/10.1016/j.envpol.2020.114575.

Zhao, B., Zheng, H., Wang, S., Smith, K.R., Lu, X., Aunan, K., et al., 2018. Change in household fuels dominates the decrease in $PM_{2.5}$ exposure and premature mortality in China in 2005–2015. Proc. Natl. Acad. Sci. Unit. States Am. 115, 12401–12406. https://doi.org/10.1073/pnas.1812955115.

Zhao, H., Geng, G., Zhang, Q., Davis, S.J., Li, X., Liu, Y., et al., 2019. Inequality of household consumption and air pollution-related deaths in China. Nat. Commun. 10, 1–9. https://doi.org/10.1038/s41467-019-12254-x.

Zheng, G.J., Duan, F.K., Su, H., Ma, Y.L., Cheng, Y., Zheng, B., et al., 2015a. Exploring the severe winter haze in Beijing: the impact of synoptic weather, regional transport and heterogeneous reactions. Atmos. Chem. Phys. 15, 2969–2983. https://doi.org/10.5194/acp-15-2969-2015.

Zheng, S., Pozzer, A., Cao, C.X., Lelieveld, J., 2015b. Long-term (2001–2012) concentrations of fine particulate matter ($PM_{2.5}$) and the impact on human health in Beijing, China. Atmos. Chem. Phys. 15, 5715–5725. https://doi.org/10.5194/acp-15-5715-2015.

Zhou, M., Wang, H., Zhu, J., 2016. Cause-specific mortality for 240 causes in China during 1990–2013: a systematic subnational analysis for the Global Burden of Disease Study 2013. Lancet 387, 251–272. https://doi.org/10.1016/S0140-6736(15)00551-6.

Zhu, G., Hu, W., Liu, Y., Cao, J., Ma, Z., Deng, Y., et al., 2019. Health burdens of ambient $PM_{2.5}$ pollution across Chinese cities during 2006–2015. J. Environ. Manag. 243, 250–256. https://doi.org/10.1016/j.jenvman.2019.04.119.